



Small scale electronic transport in diamond microcrystals

M.D. Jaeger, S. Hyun, A.R. Day¹, M.F. Thorpe, B. Golding*

Department of Physics & Astronomy and Center for Sensor Materials, Michigan State University, E. Lansing, MI 48824, USA

Abstract

The interpretation of electronic transport in polycrystalline diamond has proven difficult as a result of the disorder arising from physical and chemical inhomogeneities. We describe experimental methods, based on electron beam lithography, for studying transport in single crystallites grown by CVD on Si substrates. The electrical contacting process utilizes the flexibility of the scanning electron microscope to write metallic contacts to individual crystallites with lateral dimensions of a few μm . A detailed analysis of the current distribution in the crystals allows us to extract the electronic conductivity from arbitrarily shaped, faceted crystals. © 1997 Elsevier Science S.A.

Keywords: Small scale electronic transport; Diamond microcrystals; Electron beam lithography;

1. Introduction

Polycrystalline CVD diamond presents a number of materials challenges which must be addressed before device applications can be implemented. A major problem arises from the limited understanding of the relationships between diamond's electronic properties and its spatial and chemical inhomogeneities. For example, when grown by low-pressure deposition methods from the vapor phase, the resulting polycrystalline films contain varying amounts of sp^2 graphitic carbon bonds as well as sp^3 bonds, residual hydrogen, and impurity species. Even intentional dopants, such as boron, may not be uniformly distributed and may not occupy the same electronic states. In addition, structural defects such as growth twins are pervasive and surfaces undergo a variety of reconstructions. It is, however, the presence of grain boundaries in polycrystalline CVD material which has been implicated as a major player in degrading electronic transport properties relative to natural diamond. For example, the low-field room temperature hole mobility in single-crystal boron-doped natural diamond is quite high, $1600 \text{ cm}^2/\text{V} \cdot \text{s}$ [1], whereas polycrystalline films generally lie some two orders of magnitude below this value. The clearest evidence for the role of grain boundaries in carrier scattering has been demon-

strated in studies of highly-oriented polycrystalline diamond. Composed primarily of low-angle grain boundaries, transport measurements have shown Hall mobilities an order of magnitude higher than typical polycrystalline films containing broad distributions of large-angle crystallographic grain boundaries. [2] These studies demonstrate that even low-angle boundaries are influential in limiting hole mobilities.

In the past year we have developed experimental methods based on electron beam lithography for studying transport in *single* crystallites of CVD diamond grown on Si substrates. The crystallites are 3-dimensional, faceted, and irregularly shaped, with a typical lateral size of a few μm . The electrical contacting process makes use of a scanning electron microscope to image and expose a resist-coated crystallite in a series of lithographic operations. Since most crystallites possess a significant undercut, standard lithographic methods will result in shadowing of evaporated metal films in the regions where the diamond touches the substrate, yielding discontinuous contacts. We have therefore implemented a conformal lead metallization technique to address this problem. We present a discussion of the technique and subsequent experimental measurements of the multiterminal resistances of boron-doped diamond. An analysis of the internal electric field and current distributions has allowed us to extract the electrical conductivity from two, three, and four terminal resistance measurements.

* Corresponding author.

¹Permanent address: Physics Department, Marquette University, Milwaukee, WI 53233, USA.

2. Experiment

The process of forming electrical contacts to the microcrystallites involves multiple lithographic steps, a planarization step, and a high temperature anneal. Electron-beam lithography (EBL) is employed because it allows precise positioning of submicron contacts and leads on the micron-sized crystal facets and offers the advantage that custom electrode patterns can be easily and quickly designed for each new crystal size and shape.

Substrates for diamond microcrystallite growth were silicon wafers with a 4- μm oxide layer. The substrates are scratched using an ultrasonic treatment in a slurry of 0.1- μm diameter diamond seeds to produce low nucleation densities of order $2 \times 10^5 \text{ cm}^{-2}$. Boron-doped diamond was grown on the treated substrates using a microwave CVD technique with diborane gas as a boron source. [3] Doping levels yielded material with 1–100 $\Omega \cdot \text{cm}$ resistivity. Sufficient diamond was deposited to produce isolated crystallites 2–6 μm in diameter and 1–3 μm high primarily exhibiting $\langle 111 \rangle$ and $\langle 100 \rangle$ facets.

After diamond deposition, samples were electrochemically etched to remove surface graphite [4] and then further cleaned in an acid etch. Alignment marks were written on the substrate near each crystallite of interest to allow the positioning of contacts and leads within 0.2 μm . This was accomplished with a PMMA electron-beam resist sufficiently thick to coat the tops of the crystallites. The alignment marks were metallized with Ti/Au. Thick PMMA was then reapplied and patterned for submicron contact pads on the top facets of the diamond crystallites. Typical pad dimensions are $0.3 \mu\text{m} \times 0.3 \mu\text{m}$. PMMA residue in the developed areas is removed by a short reactive-ion etch in an oxygen plasma. The contact pads are thermally evaporated Ti/Au (15/100 nm). After lift-off, the sample is annealed in a UHV chamber above 500°C for 1 h [5]. Fig. 1 shows a simplified sequence of processing steps. Fig. 2 shows an electron micrograph of four contact pads on the surfaces of a diamond crystallite.

The system is then planarized with polyimide resin which is sufficiently thick to cover the top of the crystal. The polyimide is partially IR-cured and then isotropically wet-etched to expose the diamond tops and contact pads. PMMA is then again reapplied to the planarized landscape and EBL used to pattern 0.2- μm square Au contact wires which electrically contact the annealed Ti/Au pads and expand out to form macroscopic contacting regions.

This polyimide-planarization scheme has several advantages. The planarized landscape allows uniform PMMA thickness on top of and away from the crystallites for patterning contact leads. It also buries crystallite undercuts, thereby preventing discontinuities in contact leads caused by shadowing during lead metallization.

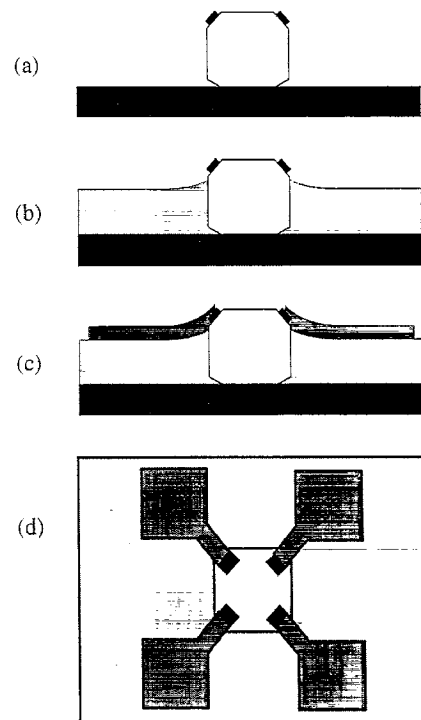


Fig. 1. Process for electron beam lithographic writing of submicron electrical contacts to a diamond microcrystallite. (a) The first EBL step creates 0.3- μm square Ti/Au pads on the upper crystal facets. (b) A thick polyimide layer planarizes the system. The polyimide is then etched to expose the top crystal facets and contact pads as shown. (c) A final EBL step creates Au leads to pads. (d) Top view of the completed structure, showing schematically four Ti/Au pads and the Au contacting leads (not to scale).

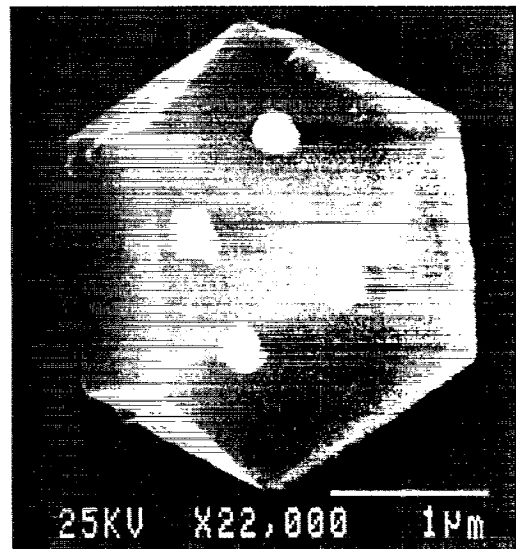


Fig. 2. Electron micrograph of a diamond micro-crystallite showing four Ti/Au contact pads.

Polyimide is well suited as a planarization polymer since it is wet-etchable, chemically inert after final cure, and electrically insulating with a high dielectric breakdown

voltage. It also acts to insulate the contact leads and macroscopic pads from possible shorts through the SiO₂ layer and is stable from cryogenic temperatures to above 450°C. An example of a “wired” sample is shown in Fig. 3.

The crystallites are connected for measurements by attaching 25- μm diameter Au wires to the large Au pads with silver paste. Since the mesoscopic leads are extremely sensitive to electrostatic discharges, care must be taken to keep the leads electrically shorted prior to use or when switching measuring instruments. Measurement currents were typically less than 10 μA , which corresponds to $2.5 \times 10^4 \text{ A cm}^{-2}$ current density in the submicron leads.

3. Results and discussion

Crystallites were characterized by I - V measurements and by temperature-dependent resistance measurements near room temperature. The I - V characteristics for good contacts were linear at the low measurement voltages ($\sim 0.2 \text{ V}$) used to measure resistances.

Because of the complex geometry, it is not straightforward to extract the electrical conductivity of the diamond sample without appreciable analysis. For four leads, the current can enter through one contact, i , and leave through another contact, j , so that there are six possible ways for the current I_{ij} to enter and leave the sample. Similarly the voltage V_{kl} can be measured across any two terminals, so that we can form a 6×6 resistance table from V_{kl}/I_{ij} .

Table 1 shows experimental results for a crystal with four contacts. A total of 36 distinct measurements of the ratio V_{kl}/I_{ij} are made. Of these, six involve two terminals only, 24 involve three terminals and six involve

Table 1

Matrix of V/I ratios in $\text{k}\Omega$ for a crystallite with sequentially labeled contacts 1–4

	I_{12}	I_{13}	I_{14}	I_{34}	I_{24}	I_{23}
V_{12}	720	569	518	-56	-231	-174
V_{13}	560	1039	540	-534	-35	499
V_{14}	508	534	986	474	498	21
V_{34}	-55	-531	477	999	531	-478
V_{24}	-232	-35	500	529	718	195
V_{23}	-176	497	20	-478	195	665

The sign of the matrix elements represents the sense of the voltage drop with respect to the lead configuration. The six two-terminal measurements are located on the diagonal. They are the largest values since they contain voltage drops due to both current contacts in addition to a voltage drop across bulk diamond. The six possible four-terminal measurements are located along the diagonals of the upper-right and lower-left 3×3 sub-matrices and are the smallest values in the matrix since they are independent of voltage drops across contacts.

all four terminals. The two or three terminal measurements include the voltage drop across common contacts in addition to the voltage drop across the diamond crystal. Typical measurement uncertainty for each element is a few $\text{k}\Omega$.

For an ohmic sample with ohmic contacts, it is straightforward to show that this resistance table should be symmetric and it can be seen that this is true to within a percent or two. It can also be shown that there are only six independent elements in the matrix, which can be chosen in many possible ways. One possible set is, perhaps surprisingly, the six diagonal elements resulting from the two-terminal measurements. It is also interesting to note that of the six four-terminal measurements, only two are independent, because of the symmetry of the matrix, and one other relationship [6].

The six independent elements will depend on the four contact resistances, geometric factors and the resistivity of the sample. We can determine the geometrical factors if we assume that the contacts are represented by series resistances with a homogenous sample described by a single resistivity ρ . Thus we have five parameters to fit to six measurements. The extra degree of freedom provides a check on the quality of the fit and hence on the above information about ρ , with one consistency check.

To obtain the geometric factors we first determine the crystal geometry by taking electron micrographs of the sample from several different projections and then by carefully measuring the coordinates of the crystal vertices and the contact pads. This information is then used to construct a three-dimensional digital image of the diamond crystal and pads. The image is optimized by using the fact that the facets of the diamond are planar and the angles between facet normals are known. Then, using a finite element package, we carry out computer simulations for the current distribution associated with

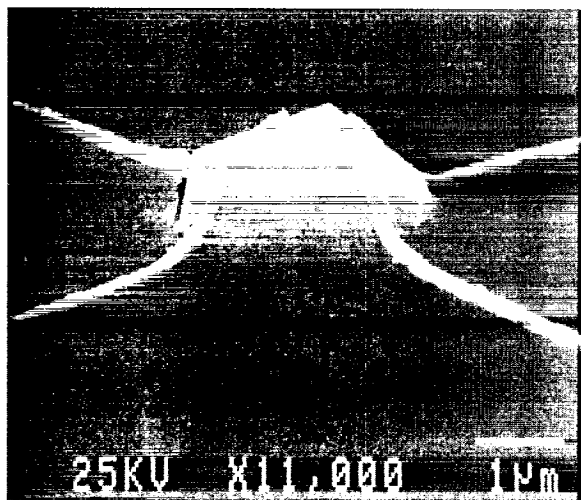


Fig. 3. Side view of top facets of a diamond crystallite extending above a polyimide planarizing layer. The four leads are conformal to the tapered surface profile.

the various elements in the resistance matrix. In the simulations we assume that the pads are perfect conductors that inject current into the sample over the area of the pad and that the voltage probes are equipotentials.

This computed resistance matrix was multiplied by the (unknown) sample resistivity ρ , and the (also unknown) contact resistances r_1 , r_2 , r_3 and r_4 were added. A least-squares fit then yielded the following results: $\rho = 22.5 \Omega \cdot \text{cm}$, $r_1 = 314 \text{ k}\Omega$, $r_2 = 15 \text{ k}\Omega$, $r_3 = 285 \text{ k}\Omega$ and $r_4 = 336 \text{ k}\Omega$. We see from these results that three contacts were of about equal quality and one was much better, with a specific contact resistivity of $10^{-5} \Omega \cdot \text{cm}^2$. With a typical sample size near $1 \mu\text{m}$, the sample resistance is about $225 \text{ k}\Omega$, which is comparable with the resistance of the contacts.

4. Conclusions

We have demonstrated the feasibility of performing reliable electron transport measurements on doped diamond microcrystals on length scales of a few μm . It has been shown that the electronic conductivity can be extracted by a suitable analysis of the current distribution within an arbitrarily shaped sample.

The procedures described above are now available to

understand the role of intergranular surfaces on the transport of carriers in diamond. It should be possible to assess the role of crystallographic orientation of the interfaces on carrier scattering as well as the effects of chemical impurities on intergranular transport. This may point the way toward methods for improving the electrical properties of polycrystalline diamond.

Acknowledgement

This work was supported by the NSF MRSEC DMR-9400417 and CFMR at Michigan State University.

References

- [1] A.T. Collins and E.C. Lightowers, in J.E. Field (ed.), *The Properties of Diamond*, Academic, London, 1979, Ch. 3, p. 86.
- [2] B.R. Stoner et al., *Appl. Phys. Lett.*, 62 (1993) 2347; D.M. Malta, J.A. von Windheim and B.A. Fox, *Appl. Phys. Lett.*, 62 (1993) 2926; D.M. Malta, J.A. von Windheim, H.A. Wynands and B.A. Fox, *J. Appl. Phys.*, 77 (1995) 1536.
- [3] Samples were grown by Kobe Steel, Research Triangle Park, NC.
- [4] M. Marchywka et al., *J. Electrochem. Soc.*, 140 (1993) L19.
- [5] H. Shiomi et al., *J. Appl. Phys.*, 28 (1989) 758.
- [6] S. Hyun, M.F. Thorpe, A.R. Day, M.D. Jaeger and B. Golding, *Phys. Rev. B*, (to be submitted).